


Article

Proton, UV, and X-ray Induced Luminescence in Tb³⁺ Doped LuGd₂Ga₂Al₃O₁₂ Phosphors

U. Fawad ^{1,2}, H. J. Kim ², Ibrahim Gul ¹, Matiullah Khan ¹, Sajjad Tahir ³ , Tauseef Jamal ⁴ and Wazir Muhammad ^{5,*}

¹ Department of Physics, Kohat University of Science & Technology, Kohat 26000, Pakistan; fawad@kust.edu.pk (U.F.); ibrahimg302@gmail.com (I.G.); dr.matiullah@kust.edu.pk (M.K.)

² Department of Physics, Kyungpook National University, Daegu 702-701, Korea; hongjoo@knu.ac.kr

³ Department of Nuclear Engineering (DNE), Institute of Engineering and Applied Sciences (PIEAS), Islamabad 45650, Pakistan; sajjadtahir@pieas.edu.pk

⁴ DCIS, Pakistan Institute Engineering and Applied Sciences (PIEAS), Islamabad 45650, Pakistan; jamal@pieas.edu.pk

⁵ Department of Physics, Charles E. Schmidt College of Science, Florida Atlantic University, Boca Raton, FL 33431-0991, USA

* Correspondence: wmuhammad@fau.edu

Received: 9 July 2020; Accepted: 16 September 2020; Published: 22 September 2020



Abstract: The well-known solid-state reaction method is used for the synthesis of Tb doped LuGd₂Ga₂Al₃O₁₂ phosphor. XRD and SEM techniques are used for the phase and structural morphology of the synthesized phosphor. UV, X-ray and proton induced spectroscopy is used to study the luminescence properties. LuGd₂Ga₂Al₃O₁₂:Tb³⁺ phosphor shows its highest peak in green and blue region. The two major emission peaks correspond to ⁵D₃→⁷F_J (at 480 to 510 nm, blue region) and ⁵D₄→⁷F_J (at 535 to 565 nm, green region). Green emission is dominant; therefore, it may be used as an efficient green phosphor. The absorption spectra of the synthesized material matches well with the spectra of light emitting diodes (LEDs); therefore, it may have applications in LEDs. X-ray spectroscopic study suggests that this phosphor may have uses in medical applications, such as X-ray imaging. The synthesized phosphor exhibits 81% efficacy in comparison to the commercial plasma display panel material (Gd₂O₂S:Tb³⁺). The Commission Internationale de l'Éclairage (CIE) chromaticity diagram is obtained for this phosphor. The decay time of ms range is measured for the synthesized phosphor.

Keywords: luminescence; phosphors; excitation; emission; sintering

1. Introduction

Rare-earth doped yttrium aluminum garnet (YAG) is a well-known commercially used phosphor due to its brilliant luminescence properties [1,2]. YAG has been studied extensively for the past few decades. LuAG is another host material that has shown promising properties due to its diverse range of properties, such as octahedral and tetrahedral structures, the transparent nature to various types of radiations, high optical quality, better thermal chemical and stability, low temperature for the synthesis, and radiation hardness [3–6].

Owing to the promising photoluminescence properties of trivalent terbium ion, contributed to green phosphors, has been investigated for last few decades. Green emission of Tb-doped borate phosphor has been investigated [7,8]. Tb doped borates (LiBaB₉O₁₅) give dominant green luminescent peak at 542 nm [9]. Tb has shown much better luminescence when doped in YAG. LuAGs possess broad peaks of emission and absorption and can be excited by blue LEDs, which make it suitable for light emitting diode (LED) applications [10–12].

$\text{LuGd}_2\text{Ga}_2\text{Al}_3\text{O}_{12}$ is one of the LuAG phases that is less studied. Therefore, this work consists of synthesis and luminescence study of Tb doped $\text{LuGd}_2\text{Ga}_2\text{Al}_3\text{O}_{12}$ phosphor.

2. Experimental

To get the phosphors' final goal, firstly, it is synthesized through solid state reaction method; a well-known technique for the synthesis of phosphors [13,14]. Lutetium oxide (Lu_2O_3 , 99.998%), gallium oxide (Ga_2O_3 , 99.99%) gadolinium oxide (Gd_2O_3 , 99.99%), and aluminum oxide (Al_2O_3) (Sigma-Aldrich, Daegu, South Korea) are weighed according to the balanced chemical equation to get a specified amount of host material $\text{LuGd}_2\text{Ga}_2\text{Al}_3\text{O}_{12}$. Different concentrations of activator, Terbium oxide (Tb_2O_3 , 99.99%), are doped with the host. Duration of ball milling, temperature, heating rate, and cooling rates are optimized for sintering the synthesized material. After measuring mass of powders it is ball milled for 7 h in order to mix it well. For sintering purpose, the mixed powders are kept in the electric furnace. The temperature of the furnace is kept constant at 700 °C for 20 h followed by slow heating and cooling rate of 100 °C/h in the air environment. Finally, fine grinded samples of Tb^{3+} doped $\text{LuGd}_2\text{Ga}_2\text{Al}_3\text{O}_{12}$ phosphors are obtained.

3. Characterizations

Scanning electron microscopy (SEM) (AIS 2000C, Seron, South Korea) is used to find the shape and size of the grains and the overall morphology of the phosphors. X-ray diffraction (XRD) (Philips XPERT-MED, Amsterdam, Netherlands) is used to find the material's crystallinity. To find luminescent properties of the synthesized material UV and X-ray induced spectroscopy (Beckman DU640 UV/Vis spectrophotometer, Kraemer Boulevard Brea, CA, USA) is used. The chromaticity diagram is obtained for the purpose of studying the white light emission. Proton beam line (45 MeV energy, 2 nA current) passes through 0.2 mm thick aluminum window, which is capping the beam pipe with 5 cm of air, loses energy up to 39 MeV [15].

Using the same spectrometer (QE65000, Ocean optics) the variation of the color with the Tb concentration is obtained using the Commission Internationale de l'Eclairage (CIE) 1931 chromaticity diagram.

4. Results and Discussion

4.1. X-ray Diffraction Analysis

XRD peaks are shown in Figure 1, which gives comparison of peaks of $\text{LuGd}_2\text{Ga}_2\text{Al}_3\text{O}_{12}:\text{Tb}^{3+}$ phosphor with $\text{Al}_5\text{Gd}_3\text{O}_{12}$ (PDF No. 98-002-3849). The peaks of our sample well match with the peaks of the reference material ($\text{Al}_5\text{Gd}_3\text{O}_{12}$). It proved that the phase achieved is the required phase for the synthesized phosphor. It also verifies that the synthesized phosphors are octahedral in structure. It is proved that extra peaks of the reactants are not present in the synthesized phosphors. It proves the single-phase phosphor material as a product. Furthermore, the Bragg's law is used for the calculation of finding lattice constants of the synthesized phosphors [16].

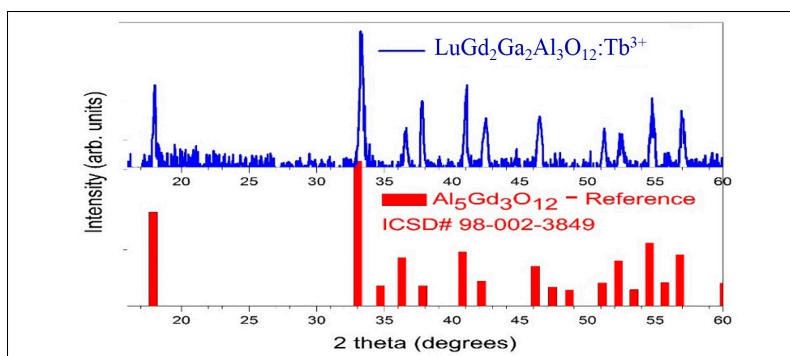


Figure 1. XRD peaks of $\text{LuGd}_2\text{Ga}_2\text{Al}_3\text{O}_{12}:\text{Tb}^{3+}$ phosphor and reference peaks of $\text{Al}_5\text{Gd}_3\text{O}_{12}$.

4.2. Scanning Electron Microscopy

The grain shape of $\text{LuGd}_2\text{Ga}_2\text{Al}_3\text{O}_{12}:\text{Tb}^{3+}$ (5 mol%) and $\text{LuGd}_2\text{Ga}_2\text{Al}_3\text{O}_{12}:\text{Tb}^{3+}$ (1 mol%) powder are shown in Figure 2. These micrographs show similar nature of grains in terms of morphology and shape. The crystallinity and the grain size in the micrometer range of the phosphor are fundamental structural properties to get high luminescence [17]. Figure 2a,b shows that $\text{LuGd}_2\text{Ga}_2\text{Al}_3\text{O}_{12}:\text{Tb}^{3+}$ (5 mol%) having small grains with irregular sharp edges, while $\text{LuGd}_2\text{Ga}_2\text{Al}_3\text{O}_{12}:\text{Tb}^{3+}$ (1 mol%) having agglomerated large grains, as shown in Figure 2. Since large grains have less chances of reflection, when the sample is exposed to light; therefore, it has better luminescence than the $\text{LuGd}_2\text{Ga}_2\text{Al}_3\text{O}_{12}:\text{Tb}^{3+}$ (5 mol%) [18]. $\text{LuGd}_2\text{Ga}_2\text{Al}_3\text{O}_{12}:\text{Tb}^{3+}$ phosphors have grain size within the micrometer range, which results in a better luminescence. Phosphors, having grain size of a micrometer, are usually used for X-ray imaging in the medical field. It is research proven that the luminescent properties of LuAG phosphors are affected by size and crystalline nature of phosphors [19,20].

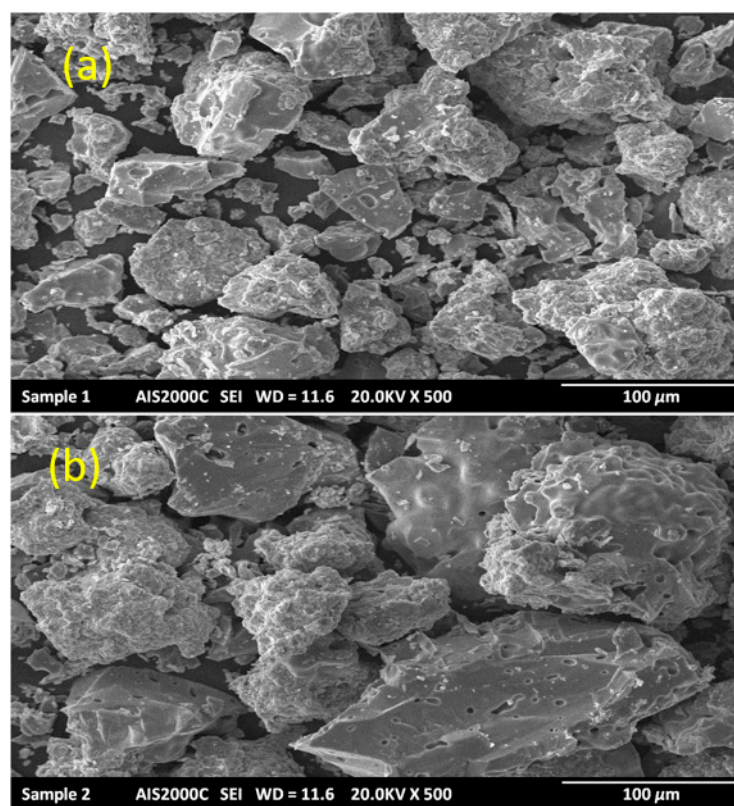


Figure 2. SEM Micrographs of (a) $\text{LuGd}_2\text{Ga}_2\text{Al}_3\text{O}_{12}:\text{Tb}^{3+}$ (5 mol%), (b) $\text{LuGd}_2\text{Ga}_2\text{Al}_3\text{O}_{12}:\text{Tb}^{3+}$ (1 mol%).

4.3. UV Induced Luminescence of $\text{LuGd}_2\text{Ga}_2\text{Al}_3\text{O}_{12}:\text{Tb}^{3+}$

Excitation and emission transitions with energy levels of Tb^{3+} ion are recorded and given in Figure 3. UV-induced excitation and emission spectra are shown in Figure 4. Excitation band of $\text{LuGd}_2\text{Ga}_2\text{Al}_3\text{O}_{12}:\text{Tb}^{3+}$ is observed at 290 nm $^7\text{F}_6 \rightarrow ^5\text{D}_3$ transition. Emission band is observed at 378 nm $^5\text{D}_4 \rightarrow ^7\text{F}_j$ transition. Where J ranges from 0 to 6.

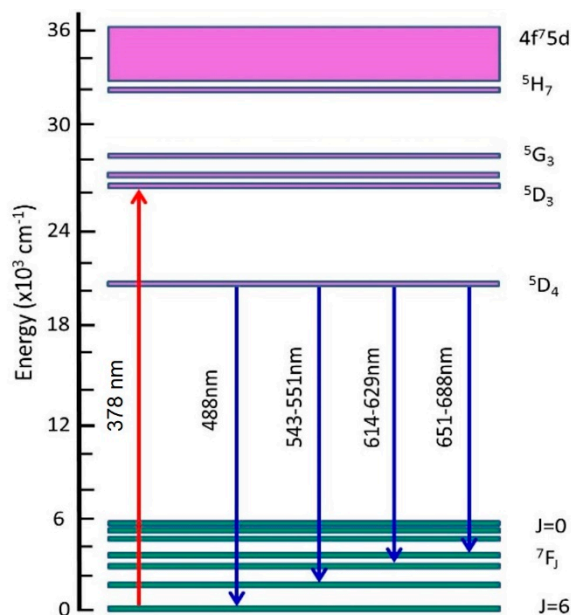


Figure 3. Energy level diagram for Tb^{3+} .

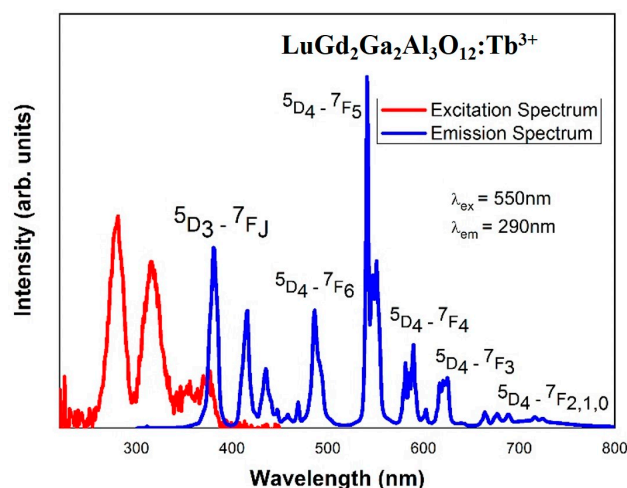


Figure 4. Excitation and Emission spectra of $LuGd_2Ga_2Al_3O_{12}:Tb^{3+}$ phosphor by UV light.

Figure 4 shows three major excitation peaks at 290 nm, 320 nm, and 378 nm. The major emission peak is observed at 550 nm. The emission spectrum of Tb^{3+} doped $LuGd_2Ga_2Al_3O_{12}$ phosphor by UV light, monitored (at the emission wavelength of 625 nm) is not limited to 550 nm, but it consists of other emission peaks at 380 nm, 420 nm, 480 nm, 580 nm, and 620 nm. Figure 4 also shows the green and blue emission spectrum of $LuGd_2Ga_2Al_3O_{12}:Tb^{3+}$ phosphor. The two major emission peaks correspond to ${}^5D_3 \rightarrow {}^7F_J$ (at 480–510 nm, blue region), ${}^5D_4 \rightarrow {}^7F_J$ (at 535–565 nm, green region). Green emission is dominant due to the presence of Tb^{3+} dopant. A similar emission is published for Tb doped phosphors [21,22]. Figure 5 shows that blue emission (${}^5D_3 \rightarrow {}^7F_J$) intensity is decreased and green emission (${}^5D_4 \rightarrow {}^7F_J$) intensity is increased with increasing concentration of Tb^{3+} . The intensity ratio (I_G/I_B) may play the same role as red/orange (I_R/I_O) intensity ratio of Eu^{3+} or yellow/blue (I_Y/I_B) intensity ratio of Dy^{3+} . It also describe the symmetry of the local environment around the optically active dopant and covalent/ ionic bonding between Tb^{3+} and O^{2-} . Similar to Eu^{3+} or Dy^{3+} , the Tb^{3+} ions may be used as a spectroscopic probe as well [23,24].

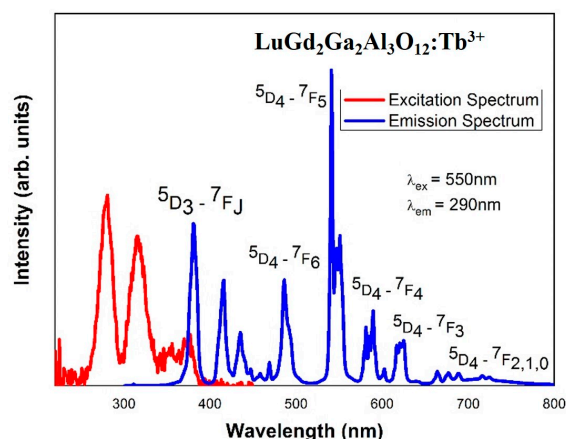


Figure 5. UV induced emission peaks of $\text{LuGd}_2\text{Ga}_2\text{Al}_3\text{O}_{12}:\text{Tb}^{3+}$ phosphor.

4.4. X-ray Induced Luminescence Spectroscopy

Emission spectra of $\text{LuGd}_2\text{Ga}_2\text{Al}_3\text{O}_{12}:\text{Tb}^{3+}$ are also observed through X-ray induced spectroscopy with various concentrations of Tb^{3+} as shown in the Figure 6.

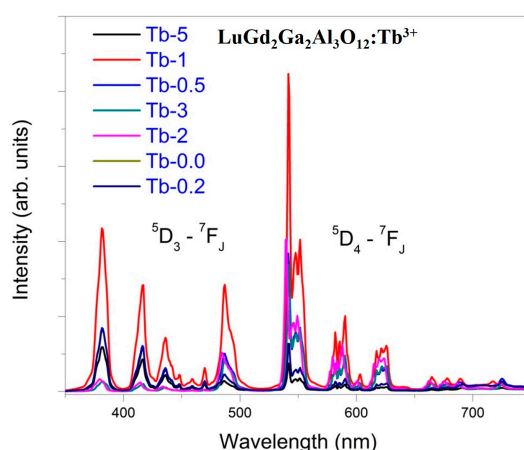


Figure 6. X-ray induced Emission spectra of $\text{LuGd}_2\text{Ga}_2\text{Al}_3\text{O}_{12}:\text{Tb}^{3+}$ phosphor.

X-ray spectroscopy shows emission in the range of 300–650 nm. X ray spectroscopy shows highest emission peak at 550 nm, which is the result of UV Spectroscopy. The X-ray induced emission spectrum well matches with that of UV induced emission spectrum and with the published data of X-ray luminescence [25]. Figure 6 shows 1 mol% concentration of Tb^{3+} in $\text{LuGd}_2\text{Ga}_2\text{Al}_3\text{O}_{12}$ as the optimized concentration of Tb^{3+} . This optimized value of 1 mol% Tb^{3+} is shown in Figure 7.

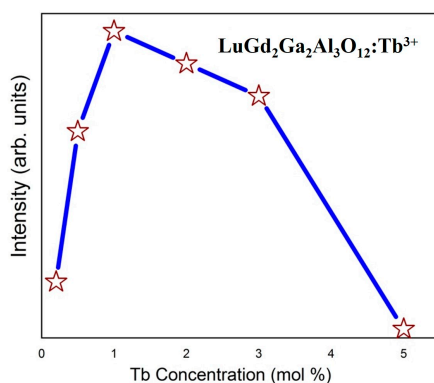


Figure 7. Optimization of Tb^{3+} concentrations in $\text{LuGd}_2\text{Ga}_2\text{Al}_3\text{O}_{12}$ host.

X-ray spectroscopic study suggests that this phosphor may be used in a medical application, such as X-ray imaging.

4.5. Optimization of Tb^{3+} Concentrations

Figure 7 shows different concentrations of Tb^{3+} (mol%) with relevant maximum emission intensities. The optimized concentrations with maximum intensity for emission peak is given, i.e., 1 mole% of Tb. Since the intensity of green color is more dominant, therefore, this phosphor might be used as green phosphor.

4.6. Proton Induced Luminescence Spectroscopy

The synthesized $LuGd_2Ga_2Al_3O_{12}:Tb^{3+}$ phosphor is excited by three major excitation sources. X-ray and proton induced emission spectra are shown in Figure 8 whereas UV-induced emission spectrum is shown in Figure 5. All three emission spectra are very similar and matches well with the literature [26,27]. This comparison shows that the emission properties do not depend on the excitation source.

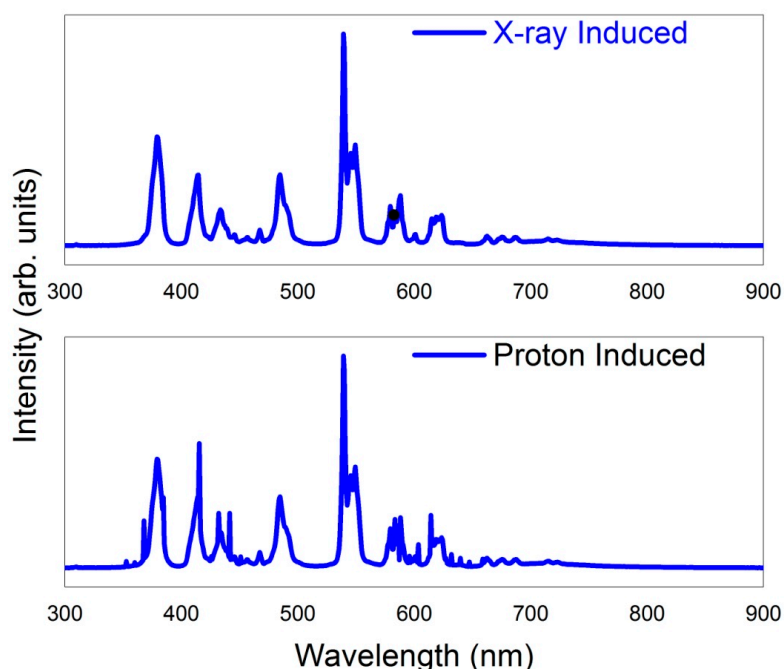


Figure 8. X-ray and proton-induced emission spectra of $LuGd_2Ga_2Al_3O_{12}:Tb^{3+}$.

4.7. Luminescence Efficiency

In order to investigate the luminescence efficacy of the synthesized phosphor, the emission spectra of $LuGd_2Ga_2Al_3O_{12}:Tb^{3+}$ and commercially available plasma display panel (PDP) material ($PDP:Gd_2O_2S:Tb^{3+}$) are compared in Figure 9. The light yields are obtained by integrating the area under the emission curves. All of the parameters, such as slit width, integrated time, beam intensity, and excitation wavelength are kept constant for comparison. This comparison reveals that the light yield of the synthesized phosphor is 81% of that of commercially available PDP phosphor. This encouraging result of luminescence efficacy suggests the potential application of this phosphor in the fields of PDPs and LEDs.

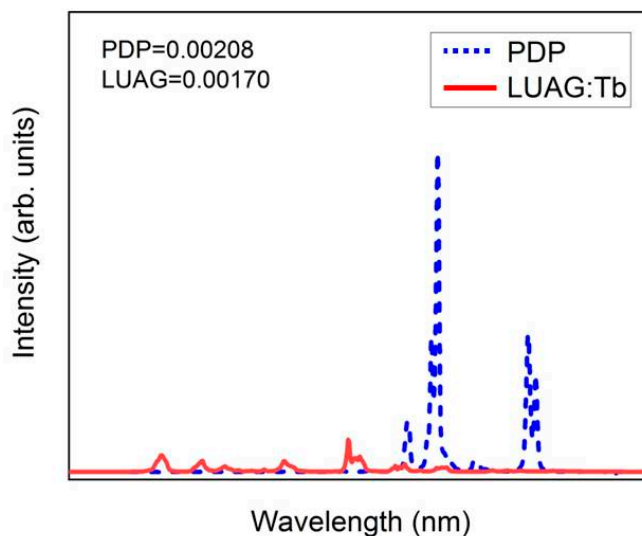


Figure 9. X-ray induced emission spectra of $\text{LuGd}_2\text{Ga}_2\text{Al}_3\text{O}_{12}:\text{Tb}^{3+}$ and plasma display panel (PDP) ($\text{Gd}_2\text{O}_2\text{S}:\text{Tb}^{3+}$).

4.8. Decay Time Analysis

The decay time is obtained for $\text{LuGd}_2\text{Ga}_2\text{Al}_3\text{O}_{12}$ phosphors with different concentrations of Tb^{3+} , shown in Figure 10. The decay measurement is done at emission wavelength (550 nm) and excitation wavelength (290 nm). All of the decay curves are fit with single exponential decay equation.

$$I = I_0 \exp(-t/\tau) \quad (1)$$

In this equation, “A” stands for integrated area, I and I_0 represent intensities at times t and 0 , respectively, and τ represents the decay time. The decay time becomes shorter with the increase of Tb^{3+} concentration. The decay time analysis is very handy in order to understand the energy transfer mechanism and luminescence quenching of Tb^{3+} ions. The investigation of these decay curves clarify that decay time gets shorter if Tb^{3+} concentration is decreased from 3 mol% to 1 mol% as mentioned in other articles [23,28]. In other words, we can say that beyond 3 mol% the concentration quenching starts, which in turn delays the emission process. The decay time measured for $\text{LuGd}_2\text{Ga}_2\text{Al}_3\text{O}_{12}:\text{Tb}^{3+}$ (1 mol%) is to be between 2.80 ms and 2.90 ms.

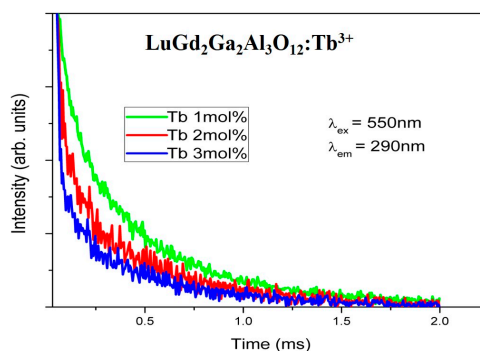


Figure 10. Decay time graph of $\text{LuGd}_2\text{Ga}_2\text{Al}_3\text{O}_{12}:\text{Tb}^{3+}$.

4.9. Chromaticity

The Commission Internationale de l’Eclairage (CIE) 1931 chromaticity diagram of $\text{LuGd}_2\text{Ga}_2\text{Al}_3\text{O}_{12}:\text{Tb}^{3+}$ is shown in Figure 11. Chromaticity is measured at three coordinates ($x_1 = 0.18$, $y_1 = 0.38$), ($x_2 = 0.2$, $y_2 = 0.39$), and ($x_3 = 0.22$, $y_3 = 0.42$) for $\text{LuGd}_2\text{Ga}_2\text{Al}_3\text{O}_{12}$ with 0.1 mol%, 1 mol%, and 5 mol% of Tb^{3+} concentrations, respectively. These values indicate that with the increase of Tb^{3+}

concentration from 0.1 mol% to 5 mol% of Tb^{3+} the bluish emission changes to greenish. This result matches well with the published materials [29].

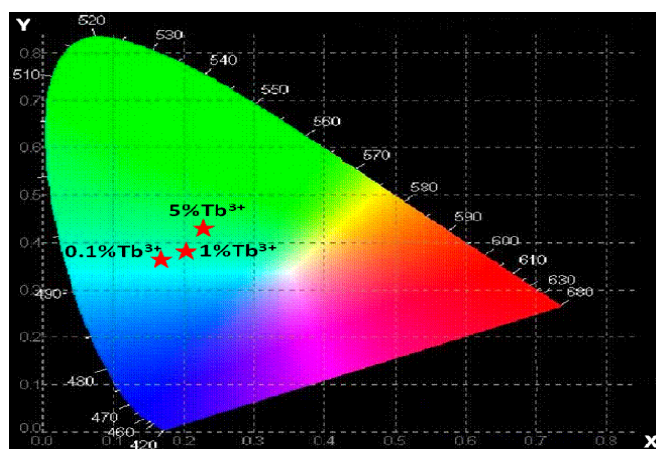


Figure 11. Chromaticity diagram of $LuGd_2Ga_2Al_3O_{12}:Tb^{3+}$ phosphors.

5. Conclusions

The synthesized phosphor is investigated for its UV, X-ray, and proton induced luminescence. All three kinds of emission spectra are very similar, proving that excitation source has no effect on the emission spectrum. This phosphor shows major emission peaks in green color region and a peak in blue region as well. The green emission enhances at the cost of blue emission with the increase of Tb concentration. Absorption spectra of our material matches well with LEDs spectra; therefore, it may be used for LED applications. Grain size is in the micrometer range, having good luminescence, and may be utilized for X-ray imaging applications. The longer decay time of this phosphor is in milliseconds range, which is suitable for lighting applications. Chromaticity diagram confirms green emission, which is supported by UV and X-ray and proton-induced spectroscopy. X-ray luminescence suggests its applications in X-ray imaging.

Author Contributions: Conceptualization, U.F. and W.M.; methodology, H.J.K.; validation, U.F. and M.K.; formal analysis, U.F., S.T. and T.J.; investigation, U.F., H.J.K. and I.G.; resources, U.F., H.J.K.; original draft preparation, U.F., M.K. and I.G.; writing—review and editing, U.F., H.J.K., I.G., M.K., S.T., T.J. and W.M.; supervision, U.F., H.J.K., M.K.; project administration, U.F.; funding acquisition, W.M. All authors have read and agreed to the published version of the manuscript.

Funding: Research reported in this publication was supported by the Department of Physics of Florida Atlantic University under Start-up Funding. The content is solely the responsibility of the authors and does not necessarily represent the official views of the Florida Atlantic University.

Conflicts of Interest: The authors declare no conflict of interest.

References

1. Tucureanu, V.; Matei, A.; Avram, A.M. Synthesis and characterization of YAG: Ce phosphors for white LEDs. *Opto-Electron. Rev.* **2015**, *2323*, 239–251.
2. Dwivedi, J.; Kumar, P.; Kumar, A.; Singh, V.N.; Singh, B.P.; Dhawan, S.K.; Shanker, V.; Gupta, B.K. A commercial approach for the fabrication of bulk and nano phosphors converted into highly efficient white LEDs. *RSC Adv.* **2014**, *4*, 54936–54947. [[CrossRef](#)]
3. Lin, S.; Zhao, X.S.; Li, Y.F. RGO-supported β -SiC nanoparticles by a facile solvothermal route and their enhanced adsorption and photocatalytic activity. *Mater. Lett.* **2014**, *132*, 380–383. [[CrossRef](#)]
4. Zorenko, Y.; Gorbenko, V.; Konstankevych, I. Single-crystalline films of Ce-doped YAG and LuAG phosphors: Advantages over bulk crystals analogues. *J. Lumin.* **2005**, *114*, 85–94. [[CrossRef](#)]
5. Park, K.; Kim, T.; Yu, Y. Y/Gd-free yellow $Lu_3Al_5O_{12}: Ce^{3+}$ phosphor for white LEDs. *J. Lumin.* **2016**, *173*, 159–164. [[CrossRef](#)]

6. Xia, Y.; Huang, X.; Wu, W. Multicolor persistent luminescence realized by persistent color conversion. *J. Lumin.* **2019**, *207*, 53–57. [[CrossRef](#)]
7. Sankar, R. Efficient green luminescence in Tb³⁺-activated borates, A₆MM'(BO₃)₆. *Opt. Mater.* **2008**, *31*, 268–275. [[CrossRef](#)]
8. Lee, T.J.; Luo, L.Y.; Diau, E.W.G. Visible quantum cutting through downconversion in green-emitting K₂GdF₅: Tb³⁺ phosphors. *Appl. Phys. Lett.* **2006**, *89*, 131121. [[CrossRef](#)]
9. Luchechko, A.; Kostyk, L.; Varvarenko, S. Green-Emitting Gd₃Ga₅O₁₂: Tb³⁺ Nanoparticles Phosphor: Synthesis, Structure, and Luminescence. *Nanoscale Res. Lett.* **2017**, *12*, 263. [[CrossRef](#)]
10. Li, G.; Cao, Q.; Li, Z. Photoluminescence properties of YAG: Tb nano-powders under vacuum ultraviolet excitation. *J. Alloys Compd.* **2009**, *485*, 561–564. [[CrossRef](#)]
11. Jain, A.; González, C.A.E.; Tejada, E.M. Covering the optical spectrum through different rare-earth ion-doping of YAG nanospheres produced by rapid microwave synthesis. *Ceram. Int.* **2018**, *44*, 1886–1893. [[CrossRef](#)]
12. Wang, Z.; Zou, J.; Zhang, C. Facile fabrication and luminescence characteristics of a mixture of phosphors (LuAG: Ce and CaAlSiN₃: Eu) in glass for white LED. *J. Non-Cryst. Solids* **2018**, *489*, 57–63. [[CrossRef](#)]
13. Van Krevel, J.W.H.; Hintzen, H.T.; Metselaar, R. Long wavelength Ce³⁺ emission in Y–Si–O–N materials. *J. Alloys Compd.* **1998**, *268*, 272–277. [[CrossRef](#)]
14. Ozuna, O.; Hirata, G.A.; McKittrick, J. Luminescence enhancement in Eu³⁺-doped α- and γ-Al₂O₃ produced by pressure-assisted low-temperature combustion synthesis. *Appl. Phys. Lett.* **2004**, *84*, 1296–1298. [[CrossRef](#)]
15. Kang, S.J.; Kim, H.J.; Hwang, Y.S. Two-dimensional beam profile monitoring by using a LYSO crystal. *J. Korean Phys. Soc.* **2010**, *56*, 2118–2121.
16. Dorset, D.L. X-ray diffraction: A practical approach. *Microsc. Microanal.* **1998**, *4*, 513–515. [[CrossRef](#)]
17. Zheng, Y.; Chen, C.; Zhan, Y. Luminescence and photocatalytic activity of ZnO nanocrystals: Correlation between structure and property. *Inorg. Chem.* **2007**, *46*, 6675–6682. [[CrossRef](#)]
18. Bi, C.; Wang, Q.; Shao, Y. Non-wetting surface-driven high-aspect-ratio crystalline grain growth for efficient hybrid perovskite solar cells. *Nat. Commun.* **2015**, *6*, 1–7. [[CrossRef](#)]
19. Rao, B.V.; Buddhudu, S. Emission analysis of RE³⁺ (Dy³⁺ or Tb³⁺): Ca₃Ln (Y,Gd)(VO₄)₃ powder phosphors. *Mater. Chem. Phys.* **2008**, *111*, 65–68.
20. Thakur, J.; Dutta, D.P.; Bagla, H. Effect of host structure and concentration on the luminescence of Eu³⁺ and Tb³⁺ in borate phosphors. *J. Am. Ceram. Soc.* **2012**, *95*, 696–704. [[CrossRef](#)]
21. Fawad, U.; Oh, M.; Park, H. Luminescent investigations of Li₆Lu (BO₃)₃: Tb³⁺, Dy³⁺ phosphors. *J. Alloys Compd.* **2014**, *610*, 281–287. [[CrossRef](#)]
22. Manohara, B.M.; Nagabhushana, H.; Sunitha, D.V. Synthesis and luminescent properties of Tb³⁺ activated cadmium silicate nanophosphor. *J. Alloys Compd.* **2014**, *592*, 319–327. [[CrossRef](#)]
23. Linganna, K.; Ju, S.; Basavapoornima, C. Luminescence and decay characteristics of Tb³⁺-doped fluorophosphate glasses. *J. Asian Ceram. Soc.* **2018**, *6*, 82–87. [[CrossRef](#)]
24. Fawad, U.; Kim, H.J.; Khan, A. X-ray and Photoluminescence Study of Li₆Gd (BO₃)₃: Tb³⁺, Dy³⁺ Phosphors. *Sci. Adv. Mater.* **2015**, *7*, 2536–2544. [[CrossRef](#)]
25. Xu, Z.; Li, Y.; Liu, Z. UV and X-ray excited luminescence of Li Tb³⁺-doped ZnGa₂O₄ phosphors. *J. Alloys Compd.* **2005**, *391*, 202–205. [[CrossRef](#)]
26. Lin, C.C.; Chen, W.T.; Chu, C.I. UV/VUV switch-driven color-reversal effect for Tb-activated phosphors. *Light Sci. Appl.* **2016**, *5*, e16066. [[CrossRef](#)]
27. Zhang, B.; Zhang, J.; Guo, Y. Synthesis and photoluminescence of double perovskite La₂LiSbO₆: Ln³⁺ (Ln = Eu, Tb, Tm, Sm, Ho) phosphors and enhanced luminescence of La₂LiSbO₆: Eu³⁺ red phosphor via Bi³⁺ doping for white light emitting diodes. *J. Alloys Compd.* **2019**, *787*, 1163–1172. [[CrossRef](#)]
28. Cheng, S.D.; Kam, C.H.; Buddhudu, S. Enhancement of green emission from Tb³⁺: GdOBr phosphors with Ce³⁺ ion co-doping. *Mater. Res. Bull.* **2001**, *36*, 1131–1137. [[CrossRef](#)]
29. Liu, X.; Yan, L.; Zou, J. Tunable cathodoluminescence properties of Tb³⁺-doped La₂O₃ nanocrystalline phosphors. *J. Electrochem. Soc.* **2009**, *157*, P1. [[CrossRef](#)]

